Energetic Passivity of the Human Ankle Joint

Hyunglae Lee, *Member, IEEE*, and Neville Hogan, *Member, IEEE*

***Abstract*—Understanding the passive or nonpassive behavior of the neuromuscular system is important to design and control robots that physically interact with humans, since it provides quantitative information to secure coupled stability while maximizing performance. This has become more important than ever apace with the increasing demand for robotic technologies in neurorehabilitation. This paper presents a quantitative characterization of passive and nonpassive behavior of the ankle of young healthy subjects, which provides a baseline for future studies in persons with neurological impairments and information for future developments of rehabilitation robots, such as exoskeletal devices and powered prostheses. Measurements using a wearable ankle robot actuating 2 degrees-of-freedom of the ankle combined with curl analysis and passivity analysis enabled characterization of both quasi-static and steady-state dynamic behavior of the ankle, unavailable from single DOF studies. Despite active neuromuscular control over a wide range of muscle activation, in young healthy subjects passive or dissipative ankle behavior predominated.**

***Index Terms*—Dissipativity, human ankle dynamics, joint mechanical impedance, passivity, physical human-robot interaction.**

I. Introduction

THE demand for rehabilitation services for people with neurological disorders is rapidly increasing with an aging population. For example, nearly 800 000 Americans experience a new or recurrent stroke each year [1], and according to the World Health Organization, 15 million people worldwide suffer stroke annually [2]. The potential to use robotic technologies to aid in the treatment of neurological disorders has grown tremendously in recent decades [3], and robotic movement therapies for restoring arm function to stroke survivors is now recommended by the American Heart Association [4] and the Department of Veterans' Affairs [5]. Robotic methods for lower-extremity rehabilitation are a critically important research area for enhancing mobility and independence. Although robotic therapies for lower-extremity rehabilitation have been extensively performed and evaluated (e.g., using Lokomat [6], [7], GaitTrainer I [8], and HapticWalker [9]), these technologies are still in development and recommendations for clinical use have not yet been achieved [4]. Much remains to be done before the great potential of robotic therapies for lower-extremity rehabilitation can be realized to the level of upper-extremity rehabilitation in clinical settings.

In addition, a number of exoskeletal devices have recently been introduced as assistive technologies for rehabilitation or to augment unimpaired human performance, for example, Cyberdine HAL [10], Ekso Bionics exoskeleton [11], ReWalk Robotics ReWalk [12], Indego [13], Sarcos XOS [14], Lockheed Martin HULC [15], MIT Exoskeleton [16], and Harvard soft exoskeleton [17]. There also have been many recent advances in the design and implementation of active prosthetic legs to restore lower-limb function in amputee patients [18]–[21].

One of the most important requirements in all of these applications in which robotic technologies operate in close physical contact with humans is to guarantee coupled stability while maximizing performance. One way to guarantee coupled stability between a robot and an arbitrary passive environment is to design and control the driving-point mechanical impedance [1] of the robot to be that of an energetically passive system [22], [23]. Driving-point impedance is the dynamic relation between input velocity (angular velocity) and output force (torque), where the scalar product of force and velocity (torque and angular velocity) determines power into the interaction port defined thereby. While most physical environments are passive, we cannot assume *a priori* that human limbs or joints are fundamentally passive, as they are controlled by active feedback neuromuscular mechanisms [24], [25]. This is especially true for individuals with neurological impairments, who commonly exhibit abnormal reflex feedback and altered muscle mechanics [26].

On the other hand, designing a robot's control system to achieve passive driving point impedance may be excessively conservative and limit performance. Less conservative designs may be achieved if a quantitative knowledge of human interactive dynamics is available [27]. In fact, as we show in the following, the ankle impedance of unimpaired humans is not merely passive, it is strongly dissipative in certain frequency ranges. This may permit even fewer conservative controller designs for physically interactive robots [28].

The human ankle plays a key role in lower-extremity motor functions [29], [30]. The objective of the study reported here was to characterize the passive (or nonpassive) behavior of the ankle, with a view to provide a baseline for future studies in persons with neurological disorders and also provide design data for exoskeletal devices and powered prostheses. In 2 degrees-of-freedom (DOF)—dorsiflexion-plantarflexion (DP)

Manuscript received August 13, 2015; revised January 07, 2016; accepted March 06, 2016. Date of publication March 10, 2016; date of current version December 06, 2016. This work was supported in part by Toyota Motor Corporation's Partner Robot Division and by the Defense Advanced Research Project Agency (DARPA) under the Warrior Web program BAA-11-72. The work of H. Lee was supported by a Samsung Scholarship. *Corresponding author: H. Lee* (e-mail: hyunglae.lee@asu.edu).

H. Lee is with the School for Engineering of Matter, Transport, and Energy, Arizona State University, Tempe, AZ 85048 USA.

N. Hogan is with the Mechanical Engineering Department and the Brain and Cognitive Science Department, Massachusetts Institute of Technology, Cambridge, MA 02139 USA (e-mail: neville@mit.edu).

Color versions of one or more of the figures in this paper are available online at http://ieeexplore.ieee.org.

Digital Object Identifier 10.1109/TNSRE.2016.2540607

[1]For brevity, we often omit the "mechanical" prefix.

and inversion-eversion (IE)—the energetic passivity (or nonpassivity) of the ankle of young healthy subjects in response to external position or torque perturbations was quantified by curl analysis [31] and passivity analysis [22], [32]. Previous work by the authors showed that the quasi-static ankle behavior of young healthy individuals with relaxed muscles is passive, evidenced by a negligible curl field [33]. In the study reported here the characterization was extended to active muscle conditions, and both quasi-static and steady-state dynamic ankle behaviors were quantified. Given the ability of healthy individuals to stably control the ankle in a variety of lower-extremity functional tasks requiring physical contact, we hypothesized that energetically nonpassive behavior of the ankle of young healthy individuals is significantly smaller than its passive or dissipative behavior even when muscles are active. A part of this work has appeared in the proceedings of a conference [34].

II. Methods

A. Subjects

In this study, two different sets of experiments were performed to characterize both quasi-static and steady-state dynamic ankle behaviors. Two groups of ten healthy individuals with no reported history of neuromuscular disorders or orthopedic limitations were recruited. One group (seven males, three females; age 19–31; height 1.55–1.80 m; weight 55.8–81.6 kg) participated in the quasi-static ankle experiment and the other group (five males, five females; age 21–37; height 1.58–1.90 m; weight 48.0–80.0 kg) participated in the steady-state dynamic ankle experiment. All protocols were approved by MIT's Committee on the Use of Humans as Experimental Subjects and written informed consent was obtained from all subjects.

B. Experimental Setup

Details of the experimental setup have been provided previously [35]. In summary, a wearable ankle robot (Anklebot, Interactive Motion Technologies Inc., Watertown, MA, USA) was used in both experiments. The robot is highly backdrivable with intrinsically low mechanical impedance and allows normal range of motion in all 3 DOFs of the foot, and 2 DOFs (IE and DP) are actively controlled. A surface electromyographic (EMG) system (Myomonitor IV, Delsys Inc., Natick, MA, USA) was used to measure activity of the ankle muscles. In addition, a visual feedback display showing the target and current levels of muscle activation was provided to help subjects voluntarily activate a specific muscle and maintain it at the target level.

Subjects were seated wearing an appropriately sized knee brace and a custom designed shoe with a mounting bracket. The robot actuators were mounted to the knee brace and their ends were connected to the shoe bracket. During measurements, the ankle was held by the robot in a neutral position, set as a right angle between the sole and the tibia. In addition, a right angle between the thigh and shank was maintained and the weight of the robot and leg was supported against gravity (Fig. 1).

Bipolar surface EMG signals were recorded from the *tibialis anterior* (TA), *peroneus longus* (PL), *soleus* (SOL), and *medial gastrocnemius* (GAS). EMG signals were amplified with a gain of 1000 and band-pass filtered between 20 and 450 Hz using fourth-order filters. Amplitudes of the EMG signals were calculated using a root-mean-square filter with a moving window of 200 ms after removing any dc component.

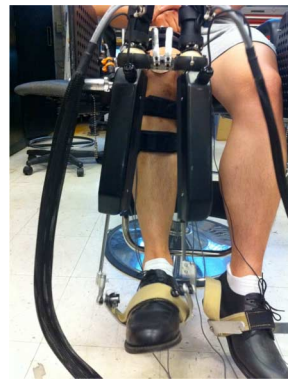

Fig. 1. Experimental setup. Subject wearing Anklebot in a seated posture.

C. Experimental Protocol

At the start of the experiment, a series of maximum voluntary contractions (MVCs) were performed based on standard muscle testing procedures [36]. The MVC level of each muscle was used as a reference to calculate normalized EMG amplitudes and set target muscle activation levels in the main experiments. In this study, two different types of measurements were made while subjects maintained nominally constant muscle activation at different target levels of TA and/or SOL.

In the quasi-static ankle experiment, the nonlinear torque-angle relationship at the ankle was identified to enable curl analysis. Measurements were made under three different muscle activations; in two of them subjects were instructed to maintain constant activation of TA or SOL at 10% MVC, and in the third condition subjects were asked to co-contract both TA and SOL at 10% MVC. SOL was selected over GAS, since GAS is a bi-articular muscle that crosses both the ankle joint and the knee joint, which may induce motions at the knee. When subjects maintained the selected target activation level, the robot applied slow ramp perturbations to the 2 DOFs of the ankle with nominal displacement amplitude of 15°. A simple impedance controller with proportional gain 200 Nm/rad and derivative gain 1 Nms/rad was used [37], and the speed of perturbations was set as 10°/s, low enough to maintain quasi-static conditions so that contributions of inertia and viscosity were minimal, and to avoid evoking stretch reflexes [38]. Each measurement consisted of a total of 24 movements along 12 equally spaced directions in IE–DP space, once outbound from the neutral position to the target position and once inbound back to the neutral position [Fig. 2(a)]. Four repetitive measurements were performed for each activation condition to minimize any possible effects due to inconstant muscle activation. A rest period of at least three minutes was given between measurements to avoid muscle fatigue. Torques and the corresponding angular displacements at the ankle in 2 DOFs and EMG data were recorded at 200 Hz.

In the steady-state dynamic ankle experiment, while subjects maintained target muscle activation levels, the robot applied mild random torque perturbations (white noise band-limited between 0 and 100 Hz) to the ankle for 40 seconds. Ankle torques

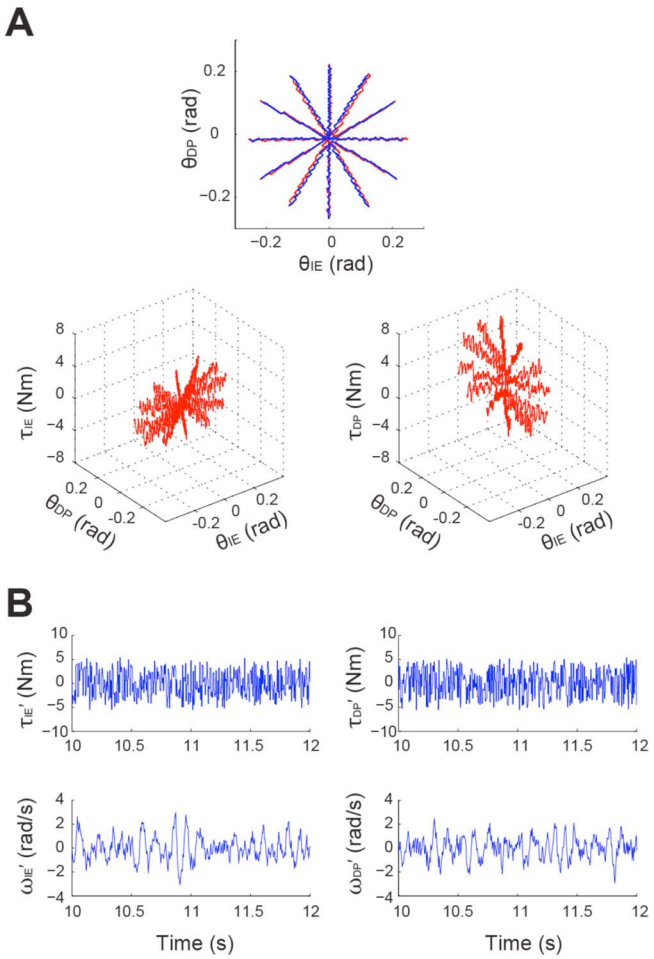

Fig. 2. Measurements for quasi-static and steady-state dynamic studies. A: Quasi-static ankle study. Top row: perturbations began with the eversion direction (0°), rotated by 30° in counter-clockwise direction on each subsequent perturbation in the IE–DP space and ended at 330°. Red and blue lines denote outbound and inbound measurements of displacements, respectively. Bottom row: angular displacements and corresponding torques in the IE–DP space for outbound data. B: Steady-state dynamic ankle study. Samples of torques and corresponding angular velocities in the IE'–DP' space (rotating the IE–DP coordinates by 45° counter-clockwise).

and angular velocities and EMG data were recorded at 1 kHz [Fig. 2(b)]. This enabled estimation of ankle impedance at frequencies up to 50 Hz with a resolution of 0.25 Hz. Measurements were made at different target levels of TA and SOL activity, from 10% to 30% MVC with increments of 5% MVC. A simple impedance controller with a proportional gain 2000 N/m (in joint coordinates, this corresponds to 37.2 and 76.0 Nm/rad for IE and DP, respectively) was implemented for each actuator to hold the ankle near its initial position against active ankle torques and combined with the random perturbations [35].

D. Analysis Methods

Curl analysis and passivity analysis were performed to investigate the passive or nonpassive behavior of the ankle. While curl analysis informs how close ankle impedance is to an energetically passive system over a considerable range of motion of the ankle (nominal displacement amplitude of 15° in IE-DP space), it is limited to the quasi-static component of ankle impedance. On the other hand, passivity analysis quantifies ankle impedance over a wide range of frequency, but only for small displacements near the neutral position of the ankle due to mild random torque perturbations (root-mean-square values were 3.3 and 2.2 Nm for DP and IE directions, respectively). Details of the methods for curl analysis and passivity analysis are fully documented in [31] and [22], respectively; brief descriptions are provided as follows.

For curl analysis, the nonlinear torque-angle relationship at the ankle in 2 DOFs was first approximated as a vector field (V)

$$(\tau_{\mathrm{IE}}, \tau_{\mathrm{DP}}) = V(\theta_{\mathrm{IE}}, \theta_{\mathrm{DP}}) \tag{1}$$

where θ_{IE} and θ_{DP} are angular displacements in the IE and DP directions, respectively, and τ_{IE} and τ_{DP} are the corresponding applied torques. The field was approximated by optimal scalar function estimation based on thin plate spline smoothing [39] with generalized cross validation [40]. This method was verified in our previous work to be sufficiently accurate to eliminate the effect of noise yet sufficiently sensitive to respond to small changes in muscle activation [33]. Before vector field approximation, torques required to overcome the friction of the actuators were identified by ten repetitive measurements following the experimental protocol explained above but without a human subject. The average of these measurements was subtracted from the measured torque. When averaged across 24 movement directions as well as across repeated trials, the mean and standard deviation (SD—shown in parentheses) of the estimated friction torques were 0.69 (0.01) Nm and 1.16 (0.01) Nm in τ_{IE} and τ_{DP}, respectively. In addition, data points around the neutral position (0–1°) and the targets (14–15°) were eliminated to remove the effect of initial lengthening and shortening of muscle fibers [41]. Four repetitive measurements in 24 directions (12 outbound, 12 inbound) were approximated separately, and outbound and inbound data were averaged into a single continuous vector field.

For sufficiently small deviations from any point in the displacement field, the torque-angle relation can be linearly approximated, and a stiffness matrix ($\boldsymbol{K}$) can be defined at that point. The stiffness matrix is further decomposed into a conservative ($\boldsymbol{K_s}$, passive) and a rotational component ($\boldsymbol{K_a}$, nonpassive) (see Appendix A), and comparison of the relative magnitudes of $\boldsymbol{K_s}$ and $\boldsymbol{K_a}$ enabled quantification of the extent to which the ankle is energetically passive. The ratio (in percentage) of the square roots of the determinants of the anti-symmetric ($\boldsymbol{K_a}$) and symmetric ($\boldsymbol{K_s}$) parts of the stiffness matrix, which may vary from 0 to ∞, was calculated to assess the relative contribution of nonzero curl components in the rotational field to the corresponding components in the conservative field

$$\sqrt{K_{\mathrm{ratio}}} = \frac{\sqrt{\det(\boldsymbol{K_a})}}{\sqrt{\det(\boldsymbol{K_s})}} \times 100. \tag{2}$$

When the rotational field has no curl, i.e., $\det(\boldsymbol{K_a}) = 0$ and accordingly $\sqrt{K_{\mathrm{ratio}}} = 0$, the torque field can be derived from

TABLE I
MEASURED MUSCLE ACTIVATIONS IN QUASI-STATIC ANKLE STUDY

Type of Study \ Muscle	TA	PL	SOL	GAS
TA Active	8.6 (0.6)	1.7 (0.7)	2.9 (0.6)	1.3 (0.8)
SOL Active	1.2 (0.9)	4.3 (2.2)	8.1 (1.3)	2.4 (1.6)
Co-contraction	9.6 (1.4)	4.0 (2.1)	8.3 (0.9)	5.2 (3.2)

Each muscle's activation level was calculated as a percentage of the corresponding MVC level. The mean and the SD (value in parentheses) over all subjects are presented.

a potential function, meaning that the system is fundamentally spring-like. The other extreme is when the field is purely described by a rotational field (zero divergence, i.e., $\det(\boldsymbol{K_s}) = 0$), which results in $\sqrt{K_{\text{ratio}}} = \infty$.

Passivity analysis provides a means to quantify passive, dissipative, and active behavior of the ankle over a range of frequencies [22], [32]. In brief, the passivity criterion for a linear n-port multi-input/multi-output (MIMO) system is described as follows (Appendix B):

$$\forall \omega \geq 0, \;\; \boldsymbol{T}(j\omega) = \boldsymbol{H}(j\omega) + \boldsymbol{H}^T(-j\omega) \geq 0$$
$$\boldsymbol{y}(j\omega) = \boldsymbol{H}(j\omega)\boldsymbol{u}(j\omega) \tag{3}$$

where ω denotes frequency and j is the complex operator. $\boldsymbol{H}$ is an $n \times n$ transfer matrix relating inputs ($\boldsymbol{u}$) and outputs ($\boldsymbol{y}$) to the system, and $\boldsymbol{u}$ and $\boldsymbol{y}$ are power conjugate variables (their inner product defines power flow into the system). If equality is restricted from (3), the system is dissipative. Linear time-invariant MIMO stochastic system identification methods [42]–[44] were used to estimate $\boldsymbol{H}$. In this study, inputs and outputs were selected in rotated joint coordinates (IE′–DP′), defined by rotating the original joint coordinates (IE–DP) by 45° counter-clockwise: $\boldsymbol{u} = \boldsymbol{\tau}' = (\tau_{IE'}, \tau_{DP'})$ and $\boldsymbol{y} = \boldsymbol{\omega}' = (\omega_{IE'}, \omega_{DP'})$, where $\boldsymbol{\tau}'$ represents torques at the interaction port, i.e., at the ankle, and $\boldsymbol{\omega}'$ denotes the corresponding angular velocities. The transformation was performed because estimates of the off-diagonal components of the transfer matrix $\boldsymbol{H}$ in the original joint coordinates were not reliable due to negligible coupling between 2 DOFs of the ankle [35], [44]. In fact, the choice of $\boldsymbol{u}$ and $\boldsymbol{y}$ is coordinate independent, since passivity analysis deals with power exchange ($\boldsymbol{u}^T\boldsymbol{y}$) at the interaction ports, where power is a scalar quantity and hence invariant under coordinate transformations. Energetic passivity or dissipativity of the ankle was assessed by evaluating whether $\boldsymbol{T}(j\omega) = [T_{11}\, T_{12};\, T_{21}\, T_{22}]$ was positive semi-definite or positive definite, respectively. More specifically, all of the leading principal minors of the $\boldsymbol{T}(j\omega)$ (T_{11} and $|T|$) were evaluated. Both T_{11} and T_{22} were checked, since the order of inputs and outputs can be arbitrarily selected (IE' first and then DP' or vice versa). In addition, as in the curl analysis, the ratio ($\sqrt{Z_{\text{ratio}}}$) of the square roots of the determinants of the anti-symmetric ($\boldsymbol{Z}_a$) and symmetric ($\boldsymbol{Z}_s$) parts of the impedance matrix ($\boldsymbol{Z}$) were calculated (in percentage) to assess the relative significance of any nonpassive behavior. The impedance matrix was estimated using torques at the ankle and corresponding angular displacements [44].

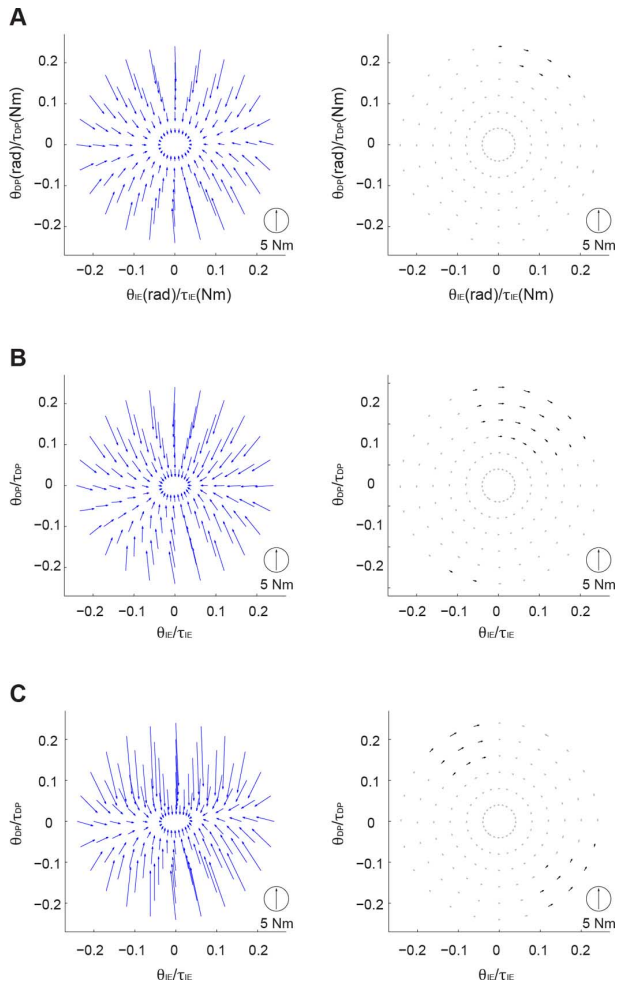

Fig. 3. Representative example of a decomposed vector field. A representative example (subject #2) of a decomposed vector field, i.e., a conservative field and a rotational (curl) field, is shown. A: TA active study, B: SOL active study, C: Co-contraction study. First and second column: conservative field and rotational (curl) field. Black lines in the rotational field denote statistically significant nonzero curl components.

III. RESULTS

A. Curl Analysis

In the quasi-static ankle study, subjects could maintain constant muscle activation around the target levels (Table I). The measured normalized TA activation levels [mean (SD) across subjects] were 8.6% (0.6%) and 9.6% (1.4%) for the TA active study and co-contraction study, respectively. Activation levels of the SOL were 8.1% (1.3%) and 8.3% (0.9%) for the SOL active study and for the co-contraction study, respectively. One subject (#1) from the SOL active study and another (#6) from

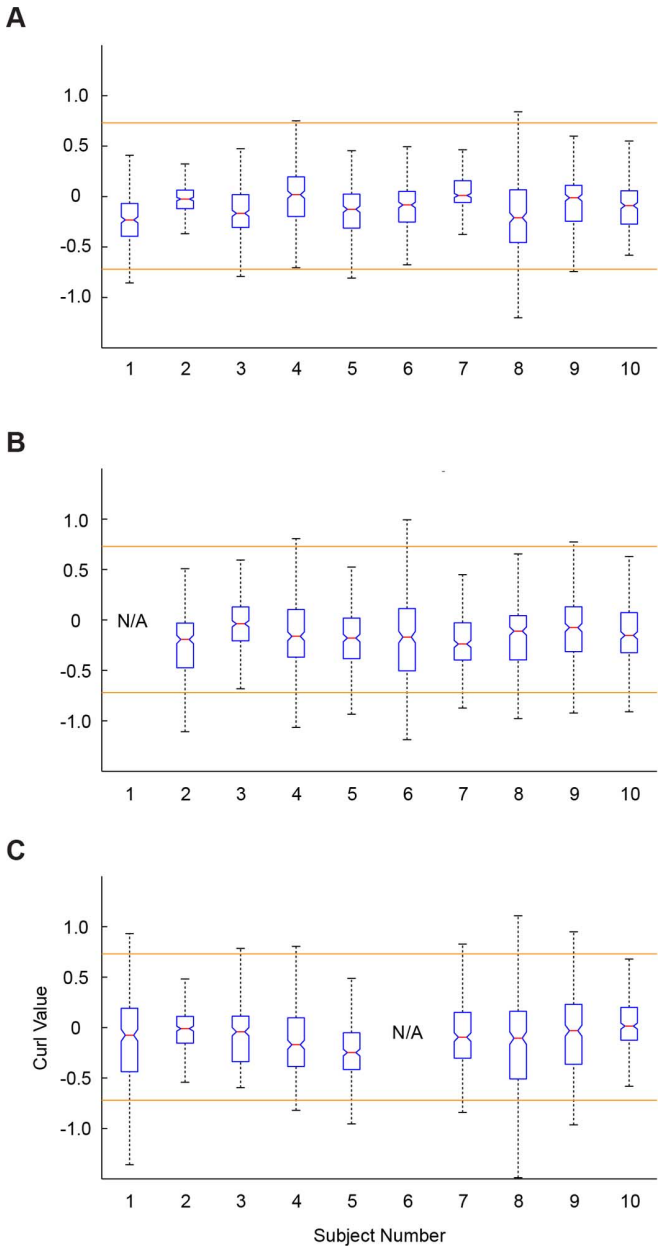

Fig. 4. Distribution of curl components for each subject. A: TA active study, B: SOL active study, C: Co-contraction study. The x-axis is the subject number and the y-axis the curl value [Unit: Nm]. In each box, the central mark is the median and the edges of the box are the 25th and 75th percentiles of all curl values, and the whiskers extend to the most extreme data points not considered outliers. Two orange lines (−0.719 and 0.728 Nm) denote the criteria for nonzero curl.

the co-contraction study exceeded the torque limit of the hardware, and their data were excluded from subsequent analysis.

Statistically significant nonzero curl was observed when muscles were active (Fig. 3). A criterion for zero curl was defined from four repetitive measurements using the same experimental protocol but unconstrained by a human subject. Ideally, a curl field (rotational field) of these measurements should be zero, since the robot was implemented as a passive system. Thus, any nonzero curl identified from the friction-compensated measurements was regarded as artifactual, due to the limited precision of measurements and/or numerical errors in differentiation. The artifactual curl components followed a normal distribution ($p > 0.05$ according to MATLAB's *jbtest* function) with 0.01 (0.37 Nm) [mean (SD)], implying that any value outside the range −0.72 to 0.73 Nm was significantly different from zero with 95% confidence. According to this criterion, significant nonzero curl components were observed in some regions of the rotational field in seven out of ten subjects for the TA active study, eight out of nine subjects for the SOL active study, and all nine subjects for the co-contraction study. However, we found no common patterns of nonzero curl, more specifically its location in the displacement field, across subjects as well as across muscle activation conditions.

TABLE II
$\sqrt{K_{\text{ratio}}}$ IN QUASI-STATIC ANKLE STUDY

Subject \ Study	TA	SOL	COC
1	11.8*	N/A	10.4*
2	9.3	17.6*	8.5*
3	11.7*	11.0	11.3*
4	10.1*	14.8*	13.7*
5	13.5*	16.0*	17.2*
6	15.0*	15.8*	N/A
7	11.5	11.4*	12.1*
8	13.2*	17.2*	13.7*
9	9.1*	10.9*	9.1*
10	9.7	9.0*	5.6*
Mean	**11.5**	**13.7**	**11.3**
(SD)	**(2.0)**	**(3.2)**	**(3.4)**

Asterisks (*) denote cases where significant non-zero curl components were observed according to the zero curl criterion.

Though significant nonzero curl was observed, the distribution of curl components for each subject showed that a large portion of the measurements fell within the zero curl criterion (Fig. 4). Group analyses across subjects further supported that curl distributions in the rotational field are statistically not significant; t-tests comparing the group data with the zero curl criterion resulted in no statistical difference in all measured conditions ($p > 0.05$). In addition, calculation of $\sqrt{K_{\text{ratio}}}$ showed that the anti-symmetric components of the stiffness matrix were substantially smaller than its symmetric components: 11.5% (2.0%), 13.7% (3.2%), and 11.3% (3.4%) for the TA active, SOL active, and co-contraction studies, respectively (Table II).

B. Passivity Analysis

In the steady-state dynamic ankle study, subjects could maintain constant muscle activation around the target levels (10%–30% MVC) in both the TA active and SOL active studies, and the correlation coefficient (R^2) of a linear fit of measured activation levels onto target levels was very high, close to 1 for both studies (Table III). The system identification used in passivity analysis was based on two assumptions that system dynamics are: 1) time-invariant and 2) linear around the neutral position of the ankle. The use of linear time-invariant system identification based on mild random torque perturbations was validated by the high percentage variance accounted for (%VAF) between output measurements and predicted outputs from identified impedances; in all measurement conditions the %VAF was higher than 84.2 (0.9)% and 89.4 (0.4)% [group

TABLE III
MEASURED MUSCLE ACTIVATIONS IN QUASI-STATIC ANKLE STUDY

Type of Study \ Target Activation Level	10% MVC	15% MVC	20% MVC	25% MVC	30% MVC	R^2
TA Active	10.8 (0.3)	15.3 (0.3)	19.9 (0.3)	24.7 (0.5)	29.8 (0.5)	0.998 (0.0002)
SOL Active	13.3 (0.7)	17.7 (0.9)	22.2 (0.8)	26.7 (0.8)	31.8 (1.0)	0.993 (0.001)

Each muscle's activation level was calculated as a percentage of the corresponding MVC level. R^2 value was calculated for each subject separately and averaged across all subjects. The mean and the SD (value in parentheses) over all subjects are presented.

TABLE IV
$\sqrt{Z_{\mathrm{ratio}}}$ IN STEADY-STATE DYNAMIC ANKLE STUDY

Subject \ Study	TA Study					SOL Study				
	10 %	**15%**	**20%**	**25%**	**30%**	**10 %**	**15%**	**20%**	**25%**	**30%**
1	14.0	7.6	3.4	4.0	6.5	4.8	11.7	4.4	8.3	8.1
2	14.6	10.5	0.2	9.8	1.1	12.8	7.8	18.7	1.7	11.8
3	8.4	16.8	4.4	5.2	6.9	4.8	3.0	5.2	7.5	4.0
4	1.2	5.0	4.2	3.4	6.6	8.5	4.7	3.3	10.7	7.6
5	8.8	6.9	6.0	4.9	5.2	26.0	10.0	8.9	14.1	1.4
6	10.0	7.2	5.0	0.6	4.2	4.4	0.6	3.6	0.4	4.9
7	4.4	9.2	4.1	1.7	5.5	4.5	2.9	1.2	0.9	11.0
8	2.0	5.0	5.0	14.8	3.7	12.3	5.6	4.6	12.2	1.1
9	9.5	1.5	4.0	10.8	10.2	11.4	15.6	5.3	7.3	12.8
10	6.3	6.8	2.1	2.8	4.1	10.4	4.5	13.9	2.7	0.2
Mean (SD)	**7.9 (4.5)**	**7.7 (4.0)**	**3.8 (1.6)**	**5.8 (4.5)**	**5.4 (2.4)**	**10.0 (6.6)**	**6.6 (4.6)**	**6.9 (5.4)**	**6.6 (4.9)**	**6.3 (4.7)**

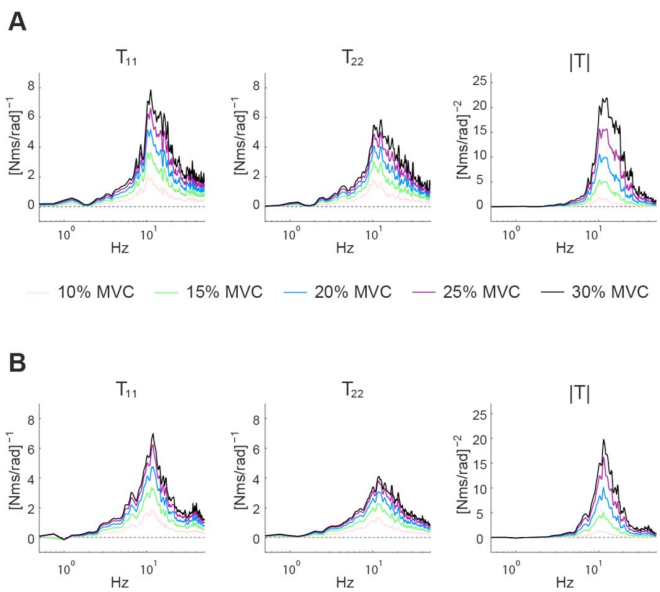

Fig. 5. Group results for passivity analysis. A: TA active study, B: SOL active study. The x-axis is operating frequency [Unit: Hz]. The mean of ten subjects for each muscle activation condition is presented.

results across subjects; mean (SD)] in DP and IE directions, respectively.

Passive or nonpassive behavior of the ankle with active muscles was quantified over a wide range of frequency. In the low-frequency region where stiffness predominates ($<\sim 2$ Hz), the ankle with active muscles was energetically passive ($\boldsymbol{T} = 0$) in most of the measurements (Fig. 5); only one subject in the TA study (#1) and three subjects in the SOL study (#2, #5, #9) exhibited active behavior ($\boldsymbol{T} < 0$) over a frequency range below about 2 Hz. Again, a criterion for passivity was defined from four repetitive measurements using the same protocol in the steady-state dynamic study but unconstrained by a human subject. In the mid-frequency range (10–20 Hz), the impedance was strictly dissipative ($\boldsymbol{T} > 0$) indicating that ankle viscosity was dominant in this region. Dissipative behavior diminished gradually at higher frequencies as inertia became dominant but the impedance remained passive (Fig. 5).

To further assess the significance of the active behavior in the low-frequency region, the ratio $\sqrt{Z_{\mathrm{ratio}}}$ was calculated below 2 Hz. In all measured conditions, the anti-symmetric components of the impedance matrix were relatively smaller than the symmetric components: when results below 2 Hz were averaged and grouped across subjects, $\sqrt{Z_{\mathrm{ratio}}}$ were less than 8% and 10% in the TA and SOL studies, respectively (Table IV).

IV. DISCUSSION

Understanding the passive or nonpassive behavior of the neuromuscular system is important, since a nonpassive system may generate energy as a function of its motion, and that may affect stability when interacting with its environment. It is important to note that the passivity tested in this study is completely distinct from the ability of a system (robot or human) to generate positive work using feedforward control. Instead, it refers to the generation of positive or negative mechanical work solely due to motion of the point(s) of contact with the environment. That is why nonpassive behavior may evoke coupled instability and why passive behavior can prevent coupled instability. This

is a particular concern for robots that physically interact with humans. Given the importance of the ankle in lower-extremity motor functions, we quantified its passive and dissipative behavior in 2 DOFs (in the sagittal and frontal planes) with active muscles.

Our main finding is that energetically passive and dissipative behaviors of the ankle of young unimpaired subjects were significantly larger than any nonpassive behavior, as we hypothesized. This is one of the reasons why humans do not exhibit the contact instability that is easily observed in robots. Passive and dissipative behavior over a wide range of frequency may have evolved as a property of the human neuromuscular system that facilitated our spectacular dexterity, agility and ability to capitalize on physical interaction with objects.

In the quasi-static ankle study, passive and nonpassive behavior of the ankle joint was identified from curl analysis of the nonlinear vector field relating torques to angular displacements. Note that this analysis is not available in single DOF studies, because curl determines the influence of displacements in one DOF on forces and torques generated in another DOF. While previous work reported that quasi-static behavior of the fully relaxed ankle is that of a passive elastic system, i.e., has zero curl [33], the study reported here demonstrated that generating a steady ankle torque or voluntarily co-contracting antagonist muscles evoked statistically significant nonpassive behavior, i.e., nonzero curl. Failure to maintain constant muscle activation might corrupt our measure of impedance and masquerade as nonzero curl. While we cannot completely rule out nonconstant muscle activation, we averaged four repeated measurements to minimize its effect on our results.

In the steady-state dynamic ankle study, passive, dissipative, and active behavior of the ankle joint was identified from analysis of the locally linear driving-point impedance of the ankle in 2 DOFs. The necessary and sufficient condition for a system such as a robot or a human limb to be stable when coupled to any stable and passive object is that its driving-point impedance should be passive [45]. Coupled stability for a robot interacting with its environment has been well addressed by controlling its impedance [46], [47]. On the other hand, we cannot assume *a priori* that human interactive behavior is fundamentally passive, since the central nervous system, from the spinal cord to the cortex, participates in feedback control of motor behavior. Unbalanced intermuscular feedback (e.g., from muscle spindles or Golgi Tendon Organs) may introduce nonpassivity [31]. The study reported here demonstrated significant nonpassive behavior of the ankle at low frequencies ($<\sim 2$ Hz) in some of the young unimpaired individuals, suggesting that it most likely originated from feedback processes. In the mid-frequency region (around 10–20 Hz) behavior was not merely passive but strongly dissipative. At still higher frequencies behavior became less dissipative, though it remained passive (Fig. 5).

For the central nervous system to maintain passive ankle impedance even when muscles were active would require any heteronymous feedback loops (from the sensors of one DOF to the muscles of another DOF) to be perfectly balanced [31]. But perfection is rare in biological systems. If the biological system had evolved to approximate passivity, albeit imperfectly, then because of individual differences in motor ability, sensory acuity, genetic factors, or other causes, we might expect individuals to differ in any departure from perfection. In fact, we found no common pattern of nonzero curl in the displacement field across subjects, consistent with individual differences in imperfect tuning of feedback circuits. Moreover, because of the delays introduced by the limited speed of neural transmission (less than ~ 120 m/s in the fastest myelinated human neurons) we might expect any nonpassivity due to imperfectly balanced neural feedback to be confined to the lowest frequencies. Indeed, our dynamic measurements showed that nonpassive behavior was confined to less than ~ 2 Hz. Taken together, these observations suggest that the human nervous system is tuned to implement passive and dissipative interactive behavior, though perhaps imperfectly.

Despite any imperfection, the nonpassive quasi-static behavior of the ankle with active muscles was quite small in these unimpaired young subjects—the group average of $\sqrt{K_{\mathrm{ratio}}}$ was less than 14% under all active conditions (Table II). Moreover, even at the lowest frequencies, the nonpassive dynamic behavior was also small—the value of $\sqrt{Z_{\mathrm{ratio}}}$ averaged over 0–2 Hz was less than 10% under all active muscle conditions (Table IV). Our observation of essentially passive behavior in the low-frequency region, dissipative behavior in the mid-frequency region, and passive behavior in the high-frequency region is consistent with previous findings that ankle impedance in each DOF is well-approximated over a wide range of muscle activation as a second-order model comprising inertia, viscosity, and stiffness [35], [48]. It further validates the 2-D spatial representation of ankle impedance presented in our previous studies (the epi-trochoidal "peanut"-shaped plots) [33], [44]. In particular, that representation depicts the magnitude of impedance for each movement direction in IE–DP space, i.e., the torques that oppose motion imposed in a particular direction, but neglects torque components orthogonal to that imposed motion, including all nonpassive components.

The results of this study provide quantitative data to inform the design of exoskeletons and powered prostheses, robotic technologies that perforce must interact physically with humans. Our data may enable superior performance because there is an intrinsic tradeoff between stability and performance in physical human-robot interaction. For example, if a human joint is strongly dissipative in a frequency range of interest, requiring a robot that interacts with it to be strictly passive may be unnecessarily conservative. The robot's mechanical impedance may be designed to be nonpassive to better utilize the robot's performance, while still maintaining robust coupled stability [27], [28].

Although we observed essentially passive and dissipative behavior in our young unimpaired subjects, that may not be the case in persons with neurological impairments, some of the potential beneficiaries of exoskeletal or prosthetic assistive technologies. In fact, we may expect substantial nonpassive behavior from this population, since the damage to descending neural pathways, such as may occur in stroke, may substantially affect both central and peripheral neural networks and cause nonpassive behavior due to altered feedback [26]. Previous studies have demonstrated that both intrinsic and reflex properties of the pathophysiological ankle impedance are altered

following stroke [49]–[52], multiple sclerosis [53], and spinal cord injury [54], substantially deviating from the unimpaired baseline. Further study of passivity or nonpassivity in persons with neurological impairments is required. The results reported here may serve as a baseline for that future work.

Together with methods developed by the authors to quantify multi-DOF joint impedance [33], [44], [55], we suggest that methods to quantify passivity or nonpassivity may add valuable information to design control strategies or treatment protocols for robot-aided neurorehabilitation. For example, if a patient exhibits energetically nonpassive behavior, the robot may compensate by being strongly dissipative to guarantee coupled stability. The robot's dissipativity could be modulated as needed, as the patient recovers and the degree of nonpassivity changes.

Lastly, it is important to note the limitations of the current study. This study was limited to time-invariant tasks and only investigated locally linear behavior of the ankle within nominal ankle displacement amplitude of 15° around a neutral ankle position. Future investigation of ankle passivity or nonpassivity in time-varying tasks, such as walking, is needed to complement current findings. In that way, we may provide better implications for the design and control of human-interactive robots and facilitate further refinement of custom-tailored neurorehabilitation.

Appendix A
Vector Field Decomposition

Although the vector field may be nonlinear for large displacements, it is approximately linear for small deviation about any point in the displacement field, given that the field is sufficiently smooth around that point $(\theta_{IE0}, \theta_{DP0})$. Torque-angular displacement relationship around a point of interest $(\theta_{IE0}, \theta_{DP0})$ can be expressed as (A1) and (A2) with Taylor series expansions

$$\delta\tau_{\mathrm{IE}} = \frac{\partial\tau_{\mathrm{IE}}}{\partial\theta_{\mathrm{IE}}}(\theta_{IE0},\theta_{DP0})\delta\theta_{\mathrm{IE}} + \frac{\partial\tau_{\mathrm{IE}}}{\partial\theta_{\mathrm{DP}}}(\theta_{IE0},\theta_{DP0})\delta\theta_{\mathrm{DP}} + H.O.T \quad \text{(A1)}$$

$$\delta\tau_{\mathrm{DP}} = \frac{\partial\tau_{\mathrm{DP}}}{\partial\theta_{\mathrm{IE}}}(\theta_{IE0},\theta_{DP0})\delta\theta_{\mathrm{IE}} + \frac{\partial\tau_{\mathrm{DP}}}{\partial\theta_{\mathrm{DP}}}(\theta_{IE0},\theta_{DP0})\delta\theta_{\mathrm{DP}} + H.O.T. \quad \text{(A2)}$$

For sufficiently small displacements from the point of interest, the higher order terms may be neglected, and the torque-angular displacement relation is linear to a first-order approximation in matrix/vector notation

$$\begin{bmatrix}\delta\tau_{\mathrm{IE}}\\ \delta\tau_{\mathrm{DP}}\end{bmatrix} = \begin{bmatrix}-K_{11} & -K_{12}\\ -K_{21} & -K_{22}\end{bmatrix}\begin{bmatrix}\delta\theta_{\mathrm{IE}}\\ \delta\theta_{\mathrm{DP}}\end{bmatrix} \quad \text{(A3)}$$

$$-K_{11} = \frac{\partial\tau_{\mathrm{IE}}}{\partial\theta_{\mathrm{IE}}} \quad -K_{12} = \frac{\partial\tau_{\mathrm{IE}}}{\partial\theta_{\mathrm{DP}}}$$
$$-K_{21} = \frac{\partial\tau_{\mathrm{DP}}}{\partial\theta_{\mathrm{IE}}} \quad -K_{22} = \frac{\partial\tau_{\mathrm{DP}}}{\partial\theta_{\mathrm{DP}}}$$
$$\delta\boldsymbol{\tau} = -\boldsymbol{K}\delta\boldsymbol{\theta}. \quad \text{(A4)}$$

The locally linearized stiffness matrix K can be further decomposed into two components, one symmetric ($\boldsymbol{K_s}$) and one anti-symmetric ($\boldsymbol{K_a}$) [see (A5)]. Superscript T denotes transpose

$$\boldsymbol{K} = \boldsymbol{K_s} + \boldsymbol{K_a}$$
$$\boldsymbol{K_s} = \frac{\boldsymbol{K}+\boldsymbol{K}^T}{2} = \begin{bmatrix}K_{11} & \frac{(K_{12}+K_{21})}{2}\\ \frac{(K_{12}+K_{21})}{2} & K_{22}\end{bmatrix}$$
$$\boldsymbol{K_a} = \frac{\boldsymbol{K}-\boldsymbol{K}^T}{2} = \begin{bmatrix}0 & \frac{(K_{12}-K_{21})}{2}\\ -\frac{(K_{12}-K_{21})}{2} & 0\end{bmatrix}. \quad \text{(A5)}$$

The symmetric part is a conservative component having zero curl. The anti-symmetric part is a rotational component having zero divergence.

Appendix B
Passivity of Linear Systems

A brief description on the passivity of LTI systems is provided. Please refer to [22] for a comprehensive review. An intuitive definition of energetic passivity is that the energy stored in the system is bounded above by the energy supplied to the system for any period of time. In a linear system, the system is passive if and only if (B1) is satisfied

$$\int_{t_1}^{t_2}\boldsymbol{u}(t)^T\boldsymbol{y}(t)dt \geq E(t_2) - E(t_1) \quad \text{(B1)}$$

$$\int_{t_1}^{t_3}\boldsymbol{u}(t)^T\boldsymbol{y}(t)dt \geq -E(t_1). \quad \text{(B2)}$$

This implies that a passive system cannot produce more energy than the initial stored energy. If the system is controllable, there exists some control such that $E(t_3) = 0$ $(t_2 < t_3 < +\infty)$ [see (B2)]. Next, by further assuming that the system is at rest as $t_1 \to -\infty$ $(E(t_1) = 0)$, the passivity criterion can be written as (B3). Especially when $\boldsymbol{u}$ and $\boldsymbol{y}$ are complex quantities, the criterion becomes

$$\int_{-\infty}^{t}\boldsymbol{u}(\tau)^T\boldsymbol{y}(\tau)d\tau \geq 0 \quad \text{(B3)}$$

$$Re\{\int_{-\infty}^{t}\boldsymbol{u}(\tau)^*\boldsymbol{y}(\tau)d\tau\} \geq 0 \quad \text{(B4)}$$

where $*$ is a Hermitian transpose operator. When $n\times n$ a transfer matrix $\boldsymbol{H}$ relating inputs ($\boldsymbol{u} = (u_1, u_2, \ldots, u_n)$) and outputs ($\boldsymbol{y} = (y_1, y_2, \ldots, y_n)$) to the system is defined, the passivity criterion can be further expressed as

$$Re\{\boldsymbol{u_0}^*\boldsymbol{H}(s)\boldsymbol{u_0}\} = \frac{1}{2}\{[\boldsymbol{u_0}^*\boldsymbol{H}(s)\boldsymbol{u_0}] + [\boldsymbol{u_0}^*\boldsymbol{H}(s)\boldsymbol{u_0}]^*\} = \boldsymbol{u_0}^*[\boldsymbol{H}(s) + \boldsymbol{H}(s)^*]\boldsymbol{u_0} \geq 0 \quad \text{(B5)}$$

where $\boldsymbol{u}(t) = \boldsymbol{u_0}e^{st}$, $\boldsymbol{y}(t) = \boldsymbol{H}(s)\boldsymbol{u_0}e^{st}$, and $s = \sigma + j\omega$. Thus, a LTI n-port is passive if and only if $\boldsymbol{H} + \boldsymbol{H}^*$ is a positive real matrix.

ACKNOWLEDGMENT

Dr. N. Hogan is a coinventor of the MIT patents for the robotic devices used in this study. He holds equity positions in Interactive Motion Technologies, Inc., the company that manufactures this type of technology under license to MIT.

REFERENCES

[1] A. S. Go *et al.*, "Heart disease and stroke statistics—2014 update Report from the American Heart Association," *Circulation*, vol. 129, pp. E28–E292, Jan. 2014.
[2] J. M. G. Mackay, "The atlas of heart disease and stroke," *World Health Org.*, 2007.
[3] H. I. Krebs and N. Hogan, "Robotic therapy: The tipping point," *Am. J. Phys. Med. Rehabil.*, vol. 91, pp. S290–S297, Nov. 2012.
[4] E. L. Miller *et al.*, "Comprehensive overview of nursing and interdisciplinary rehabilitation care of the stroke patient: A scientific statement from the American Heart Association," *Stroke*, vol. 41, pp. 2402–2448, Oct. 2010.
[5] "VA/DoD clinical practice guideline for the management of stroke rehabilitation," in *Office of Quality and Performance VA, Quality Management Division, United States Army MEDCOM (Version 3.0)*. Washington, DC, USA: Dept. of Defense, United States Dept. Veterans Affairs, American Heart Association, American Stroke Association, 2010.
[6] J. Hidler *et al.*, "Multicenter randomized clinical trial evaluating the effectiveness of the Lokomat in subacute stroke," *Neurorehabil. Neural Repair*, vol. 23, pp. 5–13, Jan. 2009.
[7] A. Mayr, M. Kofler, E. Quirbach, H. Matzak, K. Frohlich, and L. Saltuari, "Prospective, blinded, randomized crossover study of gait rehabilitation in stroke patients using the lokomat gait orthosis," *Neurorehabil. Neural Repair*, vol. 21, pp. 307–314, Jul.-Aug. 2007.
[8] S. Hesse and D. Uhlenbrock, "A mechanized gait trainer for restoration of gait," *J. Rehabil. Res. Development*, vol. 37, pp. 701–708, Nov.-Dec. 2000.
[9] H. Schmidt, C. Werner, R. Bernhardt, S. Hesse, and J. Kruger, "Gait rehabilitation machines based on programmable footplates," *J. Neuroeng. Rehabil.*, vol. 4, p. 2, 2007.
[10] H. Kawamoto and Y. Sankai, "Power assist system HAL-3 for gait disorder person," in *Proc. Int. Conf. Computers Helping People with Special Needs (Lecture Note in Computer Science)*, Linz, Austria, 2002, vol. 2398, pp. 196–203.
[11] [Online]. Available: http://www.eksobionics.com/ekso
[12] *ReWalk*, [Online]. Available: rewalk.com
[13] H. A. Quintero, R. J. Farris, and M. Goldfarb, "A method for the autonomous control of lower limb exoskeletons for persons with paraplegia," *Transact. ASME J. Medical Devices*, vol. 6, Dec. 2012.
[14] *Sarcos*, [Online]. Available: http://www.sarcos.com/
[15] *LockheedMartin*, [Online]. Available: http://www.lockheedmartin.com/products/hulc
[16] C. J. Walsh, K. Endo, and H. Herr, "A quasi-passive leg exoskeleton for load-carrying augmentation," *Int. J. Humanoid Robotics*, vol. 4, pp. 487–506, Sep. 2007.
[17] A. T. Asbeck, S. M. M. De Rossi, I. Galiana, Y. Ding, and C. J. Walsh, "Stronger, smarter, softer next-generation wearable robots," *IEEE Robotics Automation Mag.*, vol. 21, pp. 22–33, Dec. 2014.
[18] F. Sup, A. Bohara, and M. Goldfarb, "Design and control of a powered transfemoral prosthesis," *Int. J. Robotics Res.*, vol. 27, pp. 263–273, Feb. 2008.
[19] L. J. Hargrove *et al.*, "Robotic leg control with EMG decoding in an amputee with nerve transfers," *New England J. Medicine*, vol. 369, pp. 1237–1242, Sep. 2013.
[20] E. C. Martinez-Vilialpando and H. Herr, "Agonist-antagonist active knee prosthesis: A preliminary study in level-ground walking," *J. Rehabil. Res. Development*, vol. 46, pp. 361–373, 2009.
[21] S. K. Au and H. M. Herr, "Powered ankle-foot prosthesis—The importance of series and parallel motor elasticity," *IEEE Robotics Automation Mag.*, vol. 15, pp. 52–59, Sep. 2008.
[22] E. Colgate, "The Control of dynamically interacting systems," Ph.D. dissertation, Massachusetts Inst. Technology (MIT), Cambridge, MA, USA, 1988.
[23] N. Hogan and S. P. Buerger, "Impedance and interaction control," in *Robotics and Automation Handbook*. Boca Raton, FL, USA: CRC Press, 2005.
[24] D. M. Wolpert and Z. Ghahramani, "Computational principles of movement neuroscience," *Nature Neurosci.*, vol. 3, pp. 1212–1217, Nov. 2000.
[25] E. Burdet, D. W. Franklin, and T. E. Milner, "Human robotics: Neuromechanics and motor control," *Human Robotics: Neuromechanics and Motor Control*, pp. 1–277, 2013.
[26] V. Dietz and T. Sinkjaer, "Spastic movement disorder: Impaired reflex function and altered muscle mechanics," *Lancet Neurol.*, vol. 6, pp. 725–733, Aug. 2007.
[27] S. P. Buerger and N. Hogan, "Complementary stability and loop shaping for improved human-robot interaction," *IEEE Trans. Robot.*, vol. 23, no. 4, pp. 232–244, Apr. 2007.
[28] U. Nagarajan, G. Aguirre-Ollinger, and A. Goswami, "Integral admittance shaping for exoskeleton control," in *Proc. 2015 IEEE Int. Conf. Robotics and Automation*, Seattle, WA, USA, 2015.
[29] D. A. Winter, "Energy generation and absorption at the ankle and knee during fast, natural, and slow cadences," *Clin. Orthopaedics Related Res.*, pp. 147–154, 1983.
[30] J. Perry, *Gait Analysis: Normal and Pathologic Functions*. Thorofare, NJ, USA: Slack, 1992.
[31] N. Hogan, "The mechanics of multi-joint posture and movement control," *Biological Cybern.*, vol. 52, pp. 315–331, 1985.
[32] J. J. E. Slotine and W. Li, *Applied Nonlinear Control*. Englewood Cliffs, NJ, USA: Prentice Hall, 1991.
[33] H. Lee, P. Ho, M. A. Rastgaar, H. I. Krebs, and N. Hogan, "Multivariable static ankle mechanical impedance with relaxed muscles," *J. Biomechanics*, vol. 44, pp. 1901–1908, Jul. 2011.
[34] H. Lee and N. Hogan, "Essential considerations for design and control of human-interactive robots," in *Proc. IEEE Int. Conf. Robotics and Automation*, Stockholm, Sweden, 2016.
[35] H. Lee, H. I. Krebs, and N. Hogan, "Multivariable dynamic ankle mechanical impedance with active muscles," *IEEE Trans. Neural Syst. Rehabil. Eng.*, vol. 22, no. 5, pp. 971–981, Sep. 2014.
[36] J. Montgomery and D. Avers, "Daniels and Worthingham's muscle testing: Techniques of manual examination," *Saunders*, 2007.
[37] H. Lee, P. Ho, M. Rastgaar, H. I. Krebs, and N. Hogan, "Multivariable static ankle mechanical impedance with active muscles," *IEEE Trans. Neural Syst. Rehabil. Eng.*, vol. 22, no. 1, pp. 44–52, Jan. 2014.
[38] J. Lorentzen, M. J. Grey, C. Crone, D. Mazevet, F. Biering-Sorensen, and J. B. Nielsen, "Distinguishing active from passive components of ankle plantar flexor stiffness in stroke, spinal cord injury and multiple sclerosis," *Clin. Neurophysiol.*, vol. 121, pp. 1939–1951, Nov. 2010.
[39] G. Wahba, *Spline Models for Observational Data*. Philadelphia, PA, USA: Soc. Industrial Applied Mathematics, 1990.
[40] F. L. Bookstein, "Principal warps—Thin-plate splines and the decomposition of deformations," *IEEE Trans. Pattern Analysis Machine Intell.*, vol. 11, no. 6, pp. 567–585, Jun. 1989.
[41] P. M. Rack and D. R. Westbury, "The short range stiffness of active mammalian muscle and its effect on mechanical properties," *J. Physiol.*, vol. 240, pp. 331–50, Jul. 1974.
[42] E. J. Perreault, R. F. Kirsch, and A. M. Acosta, "Multiple-input, multiple-output system identification for characterization of limb stiffness dynamics," *Biological Cybern.*, vol. 80, pp. 327–337, May 1999.
[43] J. Bendat and A. Piersol, *Random Data: Analysis and Measurement Process*, 4th ed. Hoboken, NJ, USA: Wiley, 2010.
[44] H. Lee, H. I. Krebs, and N. Hogan, "Multivariable dynamic ankle mechanical impedance with relaxed muscles," *IEEE Trans. Neural Syst. Rehabil. Eng.*, vol. 22, no. 6, pp. 1104–1114, Nov. 2014.
[45] J. E. Colgate and N. Hogan, "Robust-control of dynamically interacting systems," *Int. J. Contr.*, vol. 48, pp. 65–88, Jul. 1988.
[46] N. Hogan, "Impedance control—An approach to manipulation 1. Theory," *Trans. ASME J. Dynamic Systems Measurement Control*, vol. 107, pp. 1–7, 1985.
[47] N. Hogan, "Impedance control—An approach to manipulation 3. Applications," *Trans. ASME J. Dynamic Systems Measurement Control*, vol. 107, pp. 17–24, 1985.
[48] P. L. Weiss, R. E. Kearney, and I. W. Hunter, "Position dependence of ankle joint dynamics 2. Active mechanics," *J. Biomechanics*, vol. 19, pp. 737–751, 1986.
[49] S. G. Chung, E. v. Rey, Z. Q. Bai, E. J. Roth, and L. Q. Zhang, "Biomechanic changes in passive properties of hemiplegic ankles with spastic hypertonia," *Arch. Physical Medicine Rehabil.*, vol. 85, pp. 1638–1646, Oct. 2004.
[50] S. J. Rydahl and B. J. Brouwer, "Ankle stiffness and tissue compliance in stroke survivors: A validation of myotonometer measurements," *Arch. Physical Medicine Rehabil.*, vol. 85, pp. 1631–1637, Oct. 2004.

[51] M. M. Mirbagheri, L. Alibiglou, M. Thajchayapong, and W. Z. Rymer, "Muscle and reflex changes with varying joint angle in hemiparetic stroke," *J. Neuroeng. Rehabil.*, vol. 5, p. 6, 2008.
[52] H. Lee *et al.*, "Static ankle impedance in stroke and multiple sclerosis: A feasibility study," in *Proc. Annu. Int. Conf. IEEE Engineering Medicine and Biology Soc. (EMBC)*, 2011, pp. 8523–8526.
[53] T. Sinkjaer, E. Toft, K. Larsen, S. Andreassen, and H. J. Hansen, "Non-reflex and reflex mediated ankle joint stiffness in multiple-sclerosis patients with spasticity," *Muscle Nerve*, vol. 16, pp. 69–76, Jan. 1993.
[54] M. M. Mirbagheri, H. Barbeau, M. Ladouceur, and R. E. Kearney, "Intrinsic and reflex stiffness in normal and spastic, spinal cord injured subjects," *Exp. Brain Res.*, vol. 141, pp. 446–459, Dec. 2001.
[55] H. Lee and N. Hogan, "Time-varying ankle mechanical impedance during human locomotion," *IEEE Trans. Neural Syst. Rehabil. Eng.*, vol. 22, no. 6, Nov. 2014.

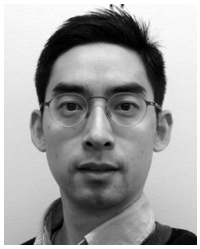

Hyunglae Lee (M'13) received the B.S. (*summa cum laude*) and M.S. degrees in mechanical engineering from Seoul National University, Seoul, Korea, in 2002 and 2004, respectively, and the Ph.D. degree in mechanical engineering from Massachusetts Institute of Technology, Cambridge, MA, USA, in 2013.

He is an Assistant Professor at the School for Engineering of Matter, Transport, and Energy, Arizona State University, Tempe, AZ, USA. He worked as a Postdoctoral Fellow at the Sensory Motor Performance Program (SMPP), Rehabilitation Institute of Chicago (RIC). He also worked at Korea Institute of Science and Technology (KIST), from 2006 to 2008, and LG Electronics, from 2004 to 2006, as a Researcher in the field of human-computer interaction, human-robot interaction, and mechanical design. His current research interests include physical human-robot interaction, rehabilitation robotics, and neuromotor control.

Dr. Lee is a recipient of Samsung Scholarship and has been awarded the 2014 Sarah Baskin Award for Excellence in Research (1st place) from RIC.

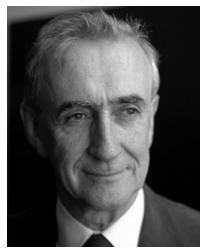

Neville Hogan (M'14) received the Dip. Eng. degree (with distinction) from the Dublin Institute of Technology, Dublin, Ireland, and the M.S., M.E., and Ph.D. degrees from Massachusetts Institute of Technology (MIT), Cambridge, MA, USA.

He is the Sun Jae Professor of Mechanical Engineering and Professor of Brain and Cognitive Sciences at MIT. Following industrial experience in engineering design, he joined MIT's school of Engineering faculty in 1979 and has served as Head and Associate Head of the MIT Mechanical Engineering Department's System Dynamics and Control Division. He is Director of the Newman Laboratory for Biomechanics and Human Rehabilitation and a Founder and Director of Interactive Motion Technologies, Inc. His research interests include robotics, motor neuroscience, and rehabilitation engineering, emphasizing the control of physical contact and dynamic interaction.

Dr. Hogan has been awarded Honorary Doctorates from Delft University of Technology and Dublin Institute of Technology; the Silver Medal of the Royal Academy of Medicine in Ireland; the Henry M. Paynter Outstanding Investigator Award, and the Rufus T. Oldenburger Medal from the Dynamic Systems and Control Division of the American Society of Mechanical Engineers.